Condensation in a Mixing Layer

Ian M. Kennedy*
University of California, Davis, Davis, California 95616

A numerical study has been carried out on the formation of a water aerosol in a laminar stagnation point flow. The two impinging streams were at different temperatures and initial supersaturations. As the streams of vapor mixed, homogeneous nucleation occurred along with condensational particle growth. Attention has been focused on the impact of the mixing rate of the two streams on the aerosol dynamics. The mixing rate is determined by the velocity gradient of the flow. High mixing rates were found to reduce the aerosol mass at the stagnation point of the flow. However, particle number densities were not affected by the velocity gradient of the flow as the aerosol dynamics adjusted themselves to the different conditions.

Nomenclature

a = velocity gradient
$\bar{c}$ = mean speed of molecule
d = diameter
f = nondimensional stream function
K = thermal conductivity
k = Boltzmann's constant
m = mass of vapor molecule
N = particle number density
P = pressure
Pr = Prandtl number
Q = volumetric heat release rate due to condensation
R = radius of cylinder
S = supersaturation
Sc = Schmidt number
T = temperature
u = velocity parallel to cylinder
v = velocity normal to cylinder
v_L = volume of molecule in liquid phase
$\dot{w}$ = reaction rate
x = distance parallel to cylinder
Y = mass fraction
y = distance normal to cylinder
β = collision rate function
η = nondimensional distance normal to cylinder
μ = viscosity
ν = kinematic viscosity
ρ = gas density
σ = surface tension

Subscripts
a = air
c = condensate
e = at edge of boundary layer
J = nucleation
p = particle
s = saturation
V = vapor
w = at wall of cylinder

Superscripts
$'$ = differentiation with respect to η
$\bar{}$ = nondimensional

Received April 11, 1990; revision received July 19, 1990; accepted for publication July 20, 1990.

*Associate Professor, Department of Mechanical Engineering. Member AIAA.

Introduction

As two streams of gas carrying a condensable vapor mix, the local supersaturation in the flow may become sufficiently high to initiate homogeneous nucleation[1,2] or heterogeneous nucleation on existing particles. Chemical reaction between vapors in the two streams may also lead to the formation of particles from a low vapor pressure product.[3] Once particles are formed, they grow by condensation of the available vapor onto their surfaces.

The production of aerosols for industrial purposes is common, and the usual concern in these operations is with the size and uniformity of the product. Atmospheric pollution may also be caused by aerosol formation. The characteristics of the aerosol are again of considerable concern for environmental and human health reasons. Particle formation and deposition on surfaces in furnaces and engines is an important technological problem[4] for which an understanding of aerosol dynamics in a mixing boundary layer is required. The visibility of the aerosol in rocket contrails is determined by the particle size and number density.[5] Many of the processes that are of interest take place in turbulent flows in which mixing occurs by turbulent transport on the large scale; at the small scales of the turbulence, molecular mixing of reactants permits chemical reactions to take place. These reactions can lead to aerosol nucleation and growth. In a similar manner, turbulent mixing of streams of gas with different partial pressures of a condensable vapor may lead to the formation of an aerosol.

The characteristics of an aerosol (i.e., number and particle size distribution) are determined by the dynamics of the nucleation, growth, and coagulation processes. The dynamics of the aerosol in a mixing flow are, in turn, associated with the rate of mixing, which is imposed upon the system by the fluid dynamics. If the characteristic rate of condensable monomer formation by chemical reaction or if the rate of aerosol growth is slow compared to a characteristic mixing rate, then the dynamics of the aerosol formation process may be altered. In a turbulent flow, the local flowfield may be resolved in terms of a translation, a rigid-body rotation, and a pure straining motion.[6] A useful analog for the straining motion in a turbulent flow is a stagnation point flow with counterflowing streams. One configuration that has received considerable attention is the flow around a porous cylinder from which a second stream of gas is emitted[7]; other stagnation point flows are kinematically similar. It is the purpose of this paper to investigate the potential impact of the flowfield in a simple, laminar flow on the dynamics of an aerosol that forms as the result of the mixing of two dissimilar streams of gas.

Stagnation Point Flow

The flow configuration that has been studied is a stagnation point flow, which is shown in Fig. 1. The model aerosol system

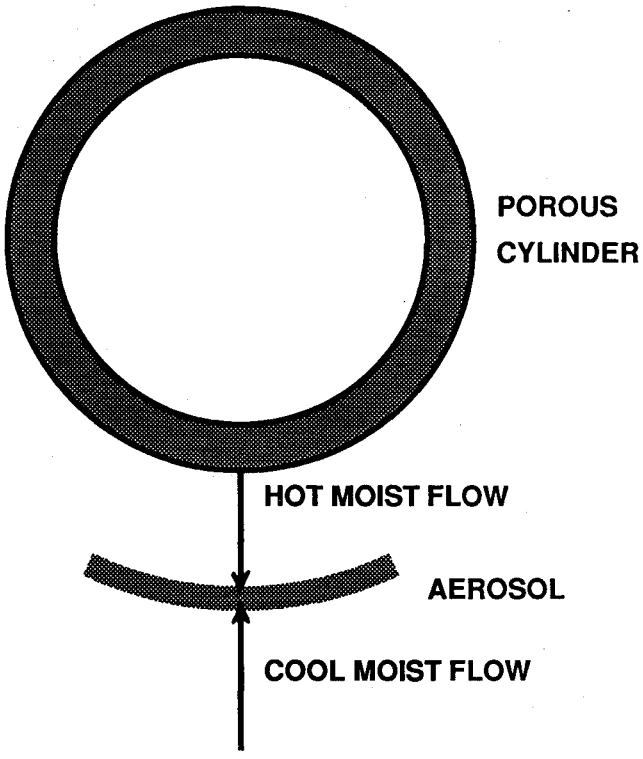

Fig. 1 Stagnation point flow.

consists of the condensation of water vapor. A warm stream of gas that is laden with water vapor issues from a porous cylinder. A cooler, water laden stream approaches the cylinder. A stagnation point is established in the flow at the front of the cylinder. This configuration was chosen in preference to an axisymmetric flow that would be produced by two impinging round jets; experimentally, the use of a porous cylinder permits filtration of one of the streams to remove foreign particles. Alteration of only a constant is required in order to convert the calculation to the kinematically similar axisymmetric case. The results that will be presented are relevant to any quasisteady strained mixing layer and are not unique to the particular configuration that has been chosen.

The straining motion of a turbulent flow can be related to the gradient in velocity of the stagnation point flow. As the strain rate or velocity gradient is increased, gradients of temperature and concentration are increased; mixing by molecular diffusion is therefore also increased. Molecular mixing in a turbulent flow is affected by the strain rate or scalar dissipation rate[8] in the same way that mixing in the laminar, stagnation point flow is affected by the velocity gradient of the flow. The laminar, stagnation point flow is useful, therefore, in understanding the effect of molecular mixing in turbulent flows.

Production of an aerosol in these flows may be affected by the mixing rate. This possibility has been explored numerically by calculating the aerosol dynamics for two different velocity gradients, $a = 10$ and $1000\ s^{-1}$, which reflect simply a change in the velocity of the flow approaching the cylinder. The nominal velocity gradient is $a = 2\ V_\infty/R$ where V_∞ is the velocity of the approaching flow well upstream of the cylinder and R is the cylinder radius.

The flow field is described by the continuity equation, momentum equation, and energy equation. In boundary-layer form, these equations are

$$\frac{\partial \rho u}{\partial x} + \frac{\partial \rho v}{\partial y} = 0 \tag{1}$$

$$\rho u \frac{\partial u}{\partial x} + \rho v \frac{\partial u}{\partial y} = \frac{\partial}{\partial y}\left(\mu \frac{\partial u}{\partial y}\right) - \frac{\partial P}{\partial x} \tag{2}$$

$$\rho u \frac{\partial T}{\partial x} + \rho v \frac{\partial T}{\partial y} = \frac{\partial}{\partial y}\left(K \frac{\partial T}{\partial y}\right) + Q \tag{3}$$

In the momentum Equation (2), the pressure gradient $\partial P/\partial x$ can be related to the velocity gradient $a = du_e/dx$ of the flow external to the viscous boundary layer. In the energy Equation (3), a constant specific heat has been assumed.

Following normal practice, the continuity equation is satisfied by writing the equations in terms of nondimensional stream function f where

$$u = u_e f'$$

$$f' = \frac{df}{d\eta}$$

$$\rho v = -(a/\rho_e \mu_e)^{1/2} f$$

The nondimensional coordinate normal to the cylinder is

$$\eta = \left(\frac{a}{\nu_e}\right)^{1/2} \int_0^y \frac{\rho}{\rho_e}\, dy^*$$

With this transformation, the momentum equation becomes an ordinary differential equation along the stagnation streamline

$$f''' + ff'' - f'^2 + \rho_e/\rho = 0 \tag{4}$$

The energy equation is rewritten in terms of a nondimensional temperature $\bar{T} = TC_P/L$, where C_P is the specific heat and L is the latent heat of vaporization. The energy equation in transformed coordinates along the stagnation streamline becomes

$$\frac{1}{Pr}\bar{T}'' + f\bar{T}' = \frac{\dot{w}}{\rho a} \tag{5}$$

These two equations describe the flow along the stagnation streamline at the front of the cylinder. They are coupled to the condensation process through the rate of condensational heat release and the density of the aerosol/gas mixture. The boundary conditions for this problem are, at the wall, $f(0) = -1$ and $T(0) = 348$ K, whereas in the freestream, $f'(\infty) = 1$ and $T(\infty) = 283$ K. The boundary condition at the wall has been chosen arbitrarily, i.e., $f(0) = -1$; variations in this value only serve to shift the zones of aerosol formation relative to the cylinder but they do not change the dynamics of the system.

Condensation

For most of the calculations that are to be discussed, no foreign particles have been introduced into the flow. Consequently, the formation of aerosol depends on the initial, homogeneous nucleation of fresh condensate material. Without the surface provided by homogeneous nucleation, further growth and condensation would be impossible.

The theory of homogeneous nucleation has been reviewed by Springer.[9] The nucleation rate that was used in these calculations was as follows:

$$J = \frac{2\ P^{1/2}\sigma^{1/2}\ v_L}{2\ \pi\ m^{1/2}k^2T^2} \exp\left[-\frac{16\ \pi}{3}\frac{v_L^2\ \sigma^3}{k^3\ T^3}\frac{1}{\ln^2 S}\right] \tag{6}$$

The dominant influences on the nucleation rate are the supersaturation S and the temperature T. In order to calculate the supersaturation, the saturated vapor pressure was calcu-

lated from Clapeyron's equation. The surface tension that appears in Eq. (6) was calculated from a curve fit to available data for water at various temperatures.

The rate of condensation onto existing particles was calculated as

$$\dot{w}_c = m \frac{\bar{c}}{4} \frac{P_s}{kT} \pi d_P^2 [S - 1] f(Kn) \tag{7}$$

where P_s is the saturation pressure and d_p is the diameter of a particle. The Kelvin effect of particle curvature has been ignored by taking particles to be created at a size somewhat larger than the critical size; Warren and Seinfeld[10] found that the size of the nuclei was not important in their calculations of aerosol dynamics. The Fuchs-Sutugin interpolation formula[11] $f(Kn)$ has been used in Eq. (7) to cover the full range of particle Knudsen numbers Kn. Particle coagulation has been handled with Schmoluchowski's formula with the assumption of a monodisperse aerosol; a size distribution could be introduced at the expense of considerably more computational effort through the use of, for example, the sectional approach of Gelbard and Seinfeld.[12] The coagulation rate is, therefore, given by

$$\dot{w}_{\text{coag}} = -\frac{\beta}{2} N^2 \tag{8}$$

where

$$\beta = 8\, kT/3\mu \tag{9}$$

The particle surface area in Eq. (7), πd_P^2, is evaluated using the assumption of a monodisperse aerosol. The particle diameter d_P may then be obtained from the condensate mass fraction Y_c, mixture density ρ, and number density N as

$$d_P = \left(\frac{6 \rho Y_c}{\pi \rho_c N} \right)^{1/3} \tag{10}$$

With the nucleation rate and condensation rate specified as in Eqs. (6) and (7), it is possible to write conservation equations for condensate mass fraction, condensable vapor mass fraction, and particle number density. The latter quantity is required in order to determine particle diameters via Eq. (10).

The equation for the mass fraction of water vapor Y_v is

$$\rho u \frac{\partial Y_v}{\partial x} + \rho v \frac{\partial Y_v}{\partial y} = \frac{\partial}{\partial y} \left(D \frac{\partial Y_v}{\partial y} \right) + \dot{w} \tag{11}$$

In transformed boundary-layer form, the equation becomes

$$\frac{1}{Sc_v} Y_v'' + f Y_v' = \dot{w}/\rho a \tag{12}$$

where the water vapor Schmidt number (ν/D) is Sc_v and the consumption rate of vapor $\dot{w}$ is the sum of two terms, i.e., $\dot{w} = \dot{w}_J + \dot{w}_c$. The rate of loss of vapor through nucleation is determined by the nucleation rate, the size of nuclei, and their density, which is taken to be the same as the bulk liquid density. At the wall of the cylinder, a balance of convection and diffusion gives

$$Y_v(0) = Y_{v_o} - \rho_w^2/\rho_e^2\, Y_v'(0)/(Sc_v \cdot f_w) \tag{13}$$

in which Y_{v_o} is the vapor mass fraction of the gas supplied to the cylinder. In the freestream,

$$Y_v(\infty) = Y_{v_\infty} \tag{14}$$

Following estimates of particle diffusivities, the Schmidt number of the condensate particles has been taken to be infinite, i.e., the particles have zero diffusivity. This has the effect of reducing the condensate mass fraction and particle number density equations to first order. The condensate mass fraction Y_c is given by

$$f Y_c' = \dot{w}/\rho a \tag{15}$$

with boundary conditions of

$$Y_c(0) = 0$$

$$Y_c(\infty) = 0$$

Similarly, the particle number density is given by

$$f N' = (J + \dot{w}_{\text{coag}})/a \tag{16}$$

with boundary conditions of

$$N(0) = 0$$

$$N(\infty) = 0$$

i.e., there are no foreign nuclei. These two equations must be integrated from either boundary of the computational domain toward the stagnation point. Hence, two boundary conditions are required for what are effectively two equations in each case. The problem is closed by specifying the density of the two-phase mixture.

Ideal gas behavior is assumed for the gaseous phases and the density of liquid water has been taken as a constant value at 300K. The mixture density is then

$$\rho = \left(\frac{Y_c}{\rho_c} + \frac{Y_v}{\rho_v} + \frac{Y_a}{\rho_a} \right)^{-1} \tag{17}$$

in which Y_a is the mass fraction of air, and the densities ρ_a and ρ_v are determined as functions of T through an ideal gas equation of state. The various mass fractions are related as

$$Y_c + Y_v + Y_a = 1 \tag{18}$$

Computations

Five simultaneous, ordinary differential equations need to be solved. They are the momentum, energy, vapor mass fraction, condensate mass fraction, and particle number density equations. The extreme sensitivity of the nucleation rate to temperature and supersaturation causes the problem to be numerically difficult. The method of solution that has been used was first developed for application to flame structure problems.[13]

The solution to the finite difference form of the equations is sought initially in a time-dependent manner to the set of equations

$$f_i(x) = 0 \tag{19}$$

As the solution to the time-dependent equations approaches sufficiently close to the steady-state solution, a damped Newton method is employed to hasten convergence by solving the system of equations

$$J_{ij}^n (\bar{x}^{n+1} - \bar{x}^n) = -\lambda^n f_i(\bar{x}^n) \tag{20}$$

where the Jacobian is

$$J_{ij} = \frac{\partial f_i}{\partial x_j} \tag{21}$$

and λ^n is the damping factor for the nth iteration. Iteration continues until the norm of the correction vector $\|\bar{x}^{n+1} - \bar{x}^n\| < 10^{-3}$. This method is able to cope with the strong nonlinearities in the condensation problem.

Results

Two velocity gradients or strain rates have been investigated. They are $a = 10$ and $1000\ s^{-1}$; this variation can be achieved in practice by adjusting the velocity of the flow approaching the cylinder by a factor of 100. The mole fraction of water vapor admitted to the porous cylinder was 0.3 for both of the cases. The supersaturation in both streams was held at unity. The nondimensional stream function at the cylinder was $f_w = -1$.

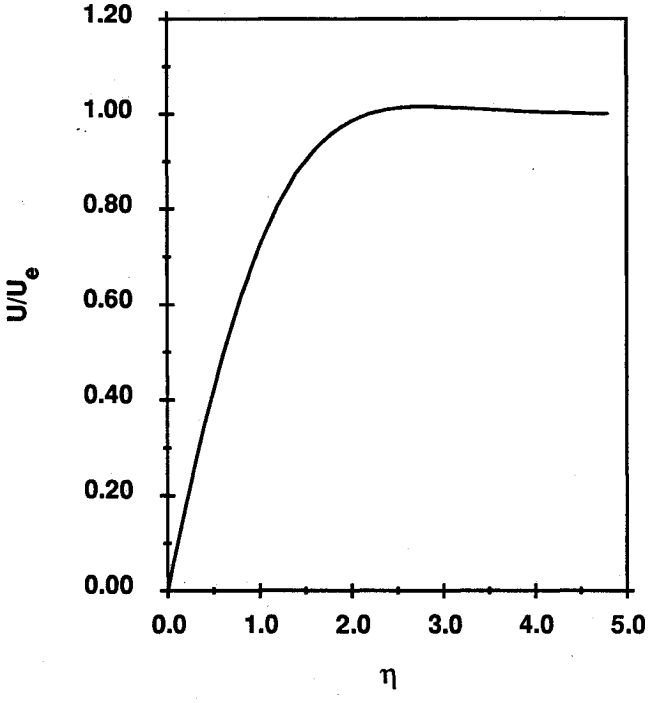

Fig. 2 Velocity profile for $a = 10\ s^{-1}$.

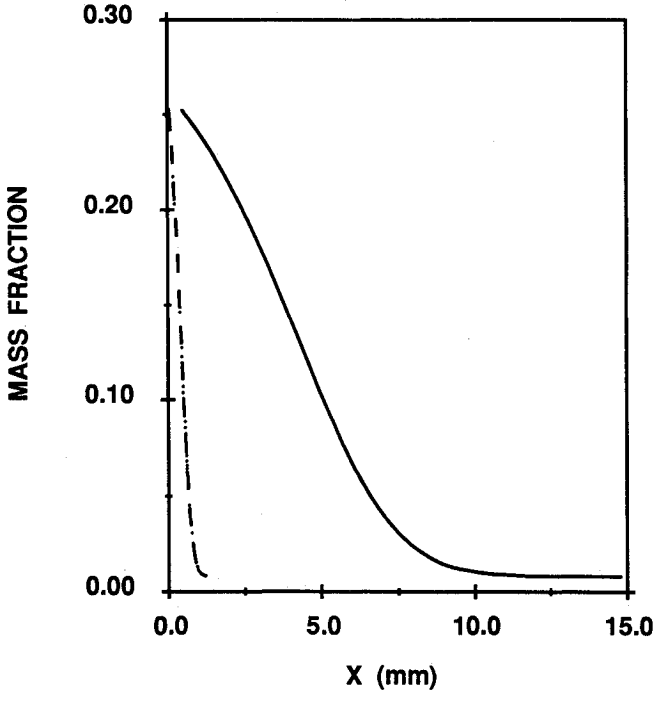

Fig. 3 Water vapor mass fractions: —— $a = 10\ s^{-1}$; --- $a = 1000\ s^{-1}$.

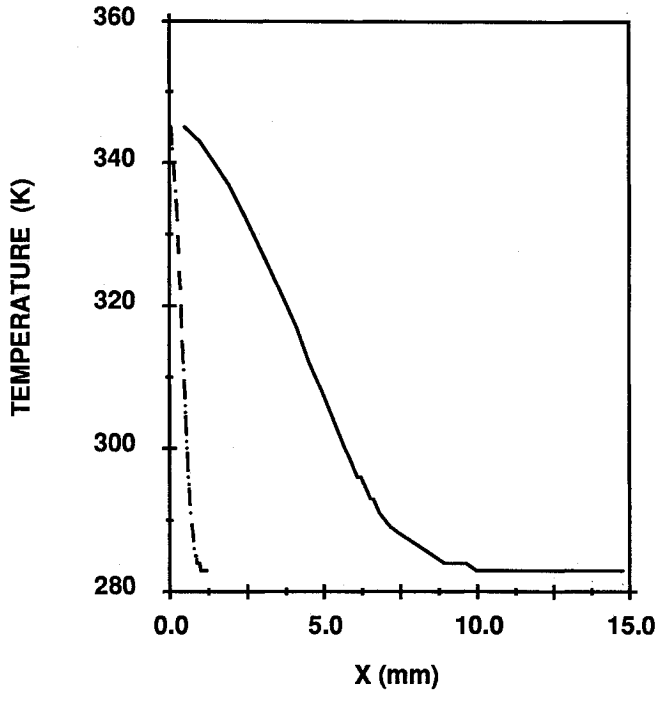

Fig. 4 Temperature profiles: —— $a = 10\ s^{-1}$; --- $a = 1000\ s^{-1}$.

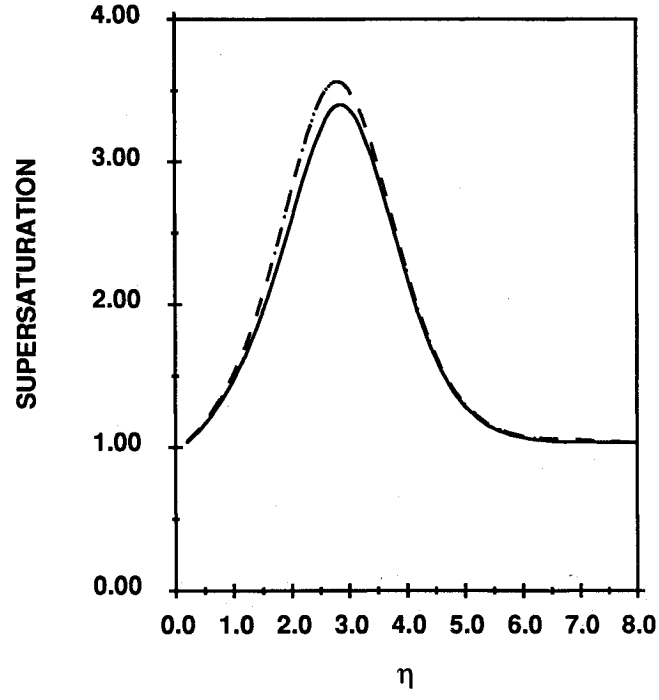

Fig. 5 Supersaturation as a function of nondimensional distance η: —— $a = 10\ s^{-1}$; --- $a = 1000\ s^{-1}$.

The flowfield for the lower velocity gradient condition ($a = 10\ s^{-1}$) is illustrated by the velocity component shown in Fig. 2. As a result, the ratio u/u_e approaches unity outside the boundary layer.

The water vapor mass fraction and temperature for both cases are shown in Figs. 3 and 4, respectively, as functions of dimensional distance. Because the Lewis number is close to 1, the profiles of Y_v at a given velocity gradient are similar to those of T. The effect of increased blowing is to cause a significant steepening of the thermal and concentration gradients. If Figs. 3 and 4 were replotted in terms of the similarity coordinate η, then the curves for different values of velocity gradient a would be almost identical. Presentation of the re-

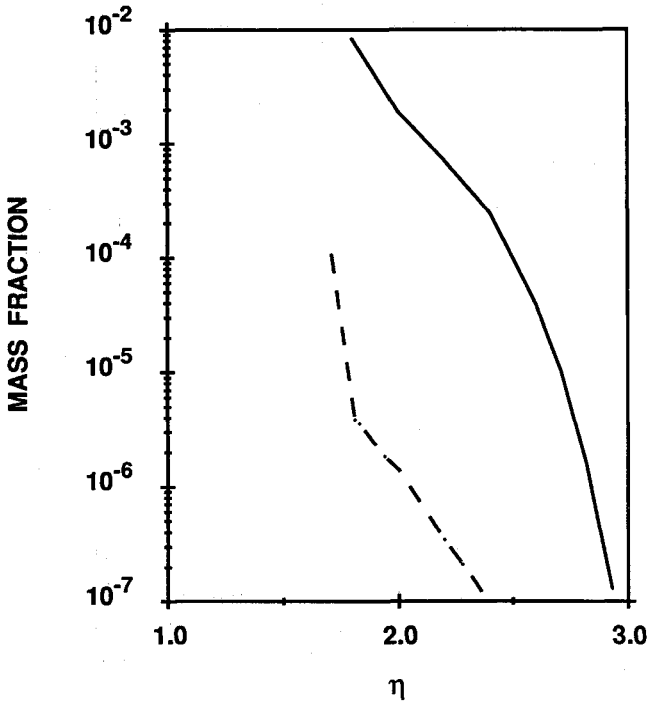

Fig. 6 Aerosol mass fractions as a function of nondimensional distance η: —— $a = 10\ s^{-1}$; --- $a = 1000\ s^{-1}$.

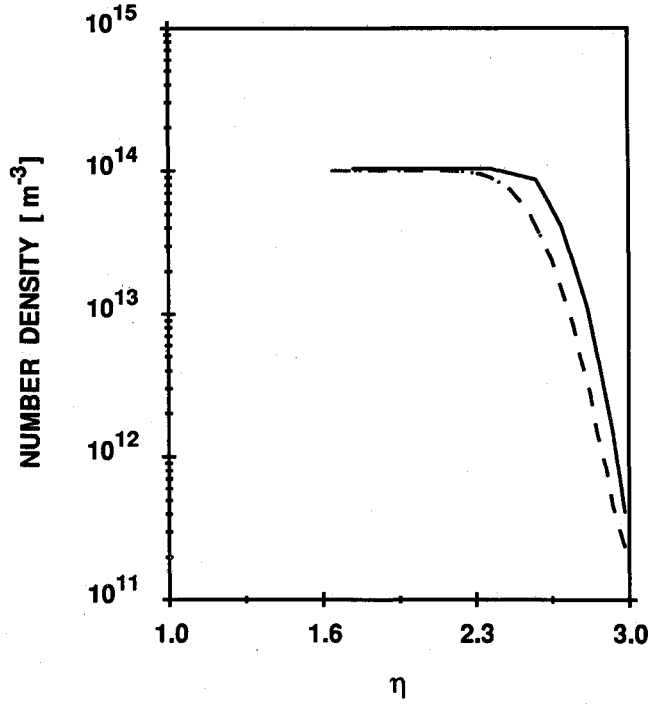

Fig. 7 Particle number densities as a function of nondimensional distance η: —— $a = 10\ s^{-1}$; --- $a = 1000\ s^{-1}$.

sults in terms of the nondimensional similarity coordinate facilitates comparisons of the results for different flow conditions and, therefore, is used in the following discussion.

The supersaturations for both flows ($a = 10$ and $1000\ s^{-1}$) are presented in Fig. 5 as functions of the nondimensional distance η. It is apparent that blowing harder against the cylinder causes the peak supersaturation for $a = 1000\ s^{-1}$ to be about 3.56 compared to a value of 3.40 for the lower velocity gradient. The reason for this behavior will be explained later.

Figure 6 presents the condensate mass fraction for the two flows. Increasing the velocity gradient has the effect of reducing the amount of condensate that is formed. This is not unexpected since the characteristic residence time for the aerosol in the flow is given by $1/a$; less residence time leads to less condensation.

Figure 7 shows the particle number densities for the two velocity gradients. In this figure, it is apparent that an increase in the velocity gradient has little effect on the number density of particles near the stagnation point, even though, as we shall see, the particle nucleation rate is affected substantially. Of course, the aerosol zone in the flow is much thinner (by

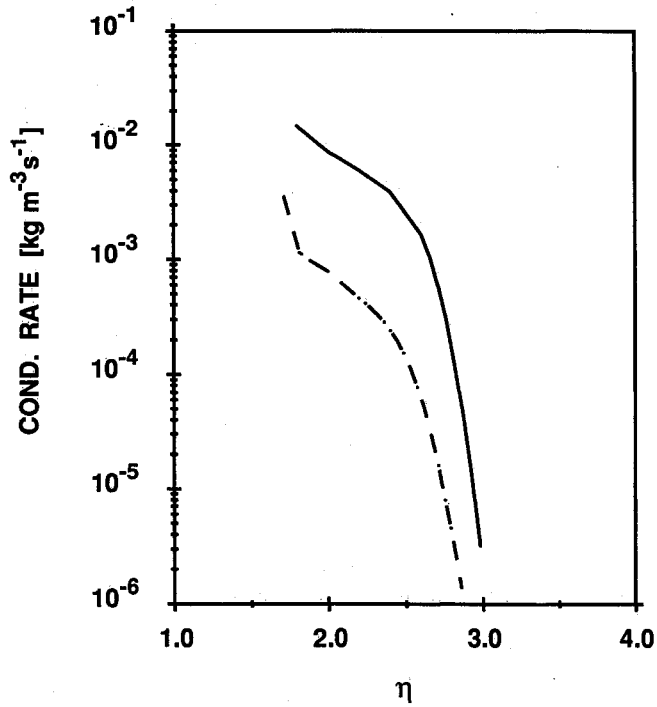

Fig. 8 Condensation rates as a function of nondimensional distance η: —— $a = 10\ s^{-1}$; --- $a = 1000\ s^{-1}$.

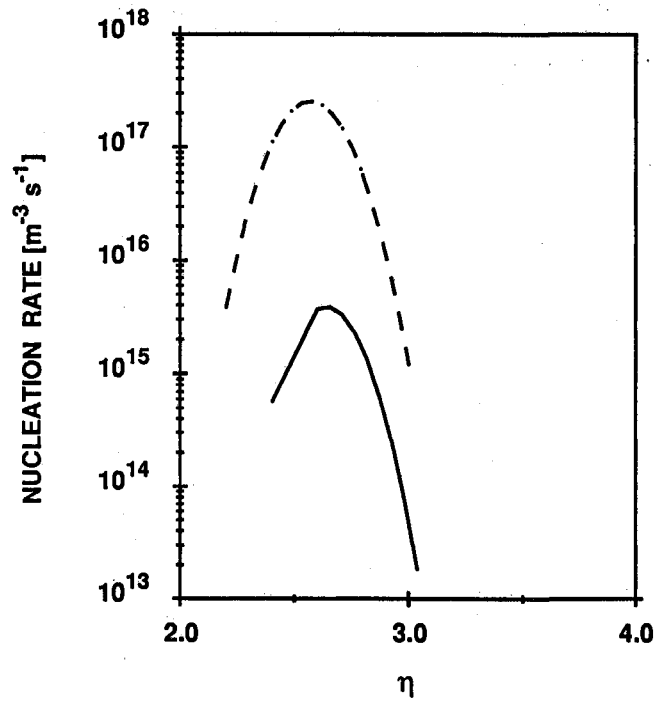

Fig. 9 Nucleation rates as a function of nondimensional distance η: —— $a = 10\ s^{-1}$; --- $a = 1000\ s^{-1}$.

an order of magnitude) at the higher velocity gradient; this would be apparent in a plot of the same results as a function of physical distance from the cylinder. Coagulation serves to keep number densities about the same, and, in addition, higher nucleation rates at higher velocity gradients are offset by reduced residence times for the flow. Condensation rates onto droplets and nucleation rates of fresh particles are shown in Figs. 8 and 9, respectively. A significant effect of the mixing rate or velocity gradient may be seen for both of the rates.

The effect of pre-existing particles on the dynamics of the aerosol processes has been investigated by altering the boundary conditions at the cylinder and at the freestream boundary.

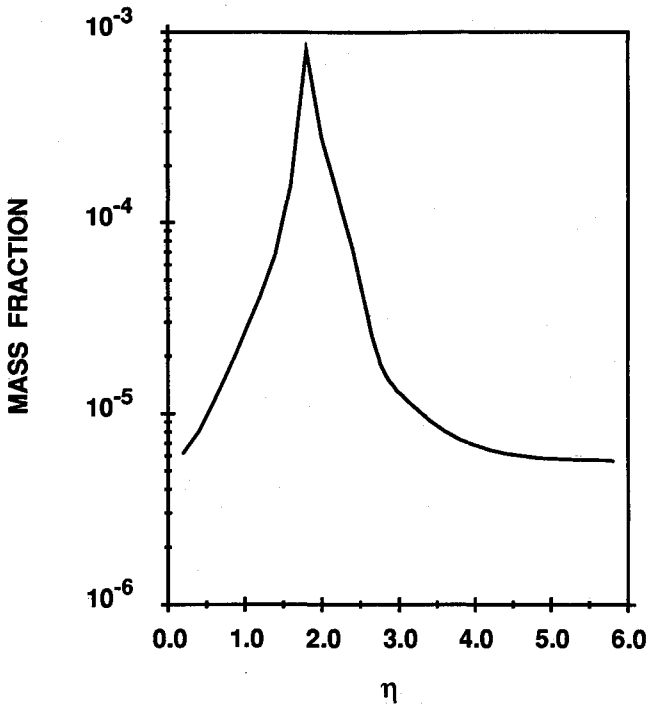

Fig. 10 Aerosol mass fraction with particles in the freestreams, a = 10 s^{-1}.

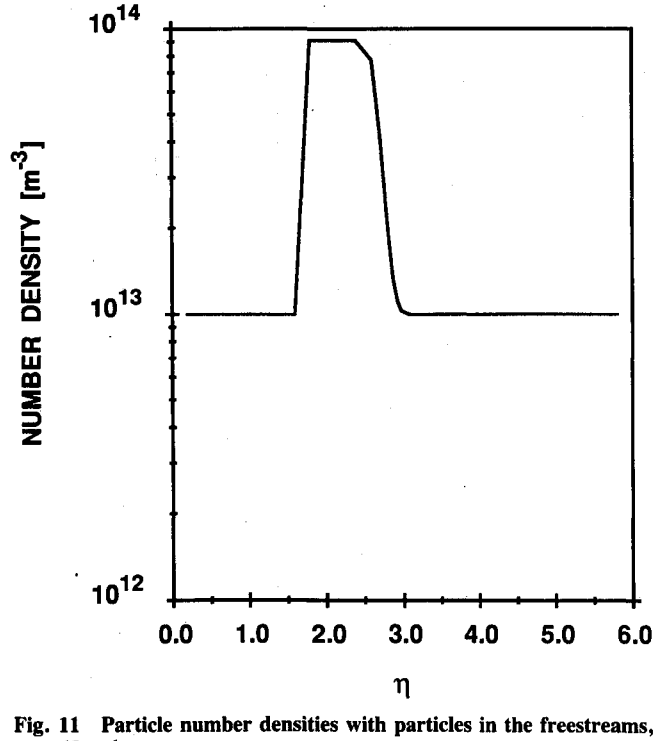

Fig. 11 Particle number densities with particles in the freestreams, a = 10 s^{-1}.

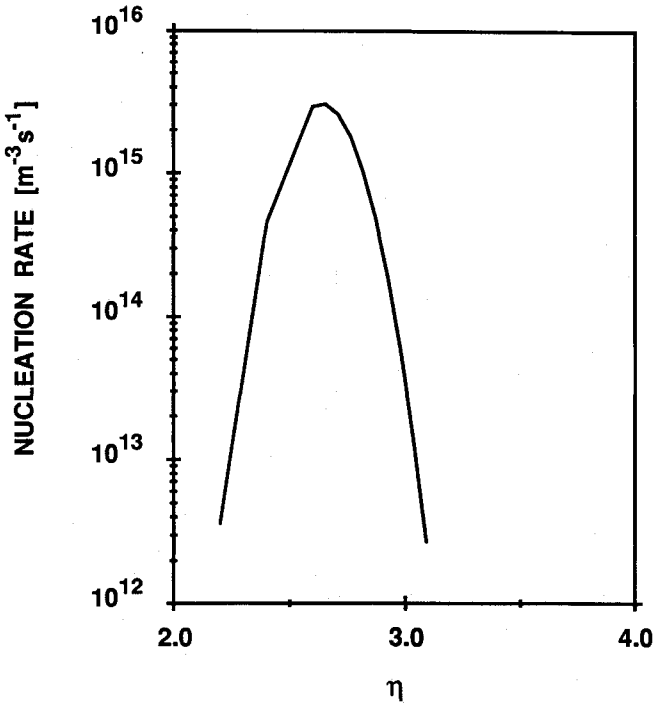

Fig. 12 Nucleation rate with particles in the freestreams, a = 10 s^{-1}.

Particle number densities of 10^{13} m^{-3} have been prescribed with particle diameters of 125 nm; the particles are assumed to be water so that there is no alteration to the surface condensation rates. Because the vapor supersaturations are unity in both of the streams, outside the mixing layer there is no condensational growth or evaporation of the droplets prior to their arrival at the stagnation region of the flow.

Pre-existing particles or foreign nuclei may have substantial effects on aerosol formation dynamics by serving to scavenge vapor and reduce supersaturation levels. By this means, heterogeneous nucleation or condensational growth may be favored over homogeneous nucleation. Figure 10 presents the condensate mass fraction for a velocity gradient of 10 s^{-1}. The maximum amount of condensate at the stagnation point is somewhat lower than that obtained with particle free boundary conditions. The number densities that are shown in Fig. 11 indicate that the peak number density at the stagnation point is slightly lower than in the original calculation shown in Fig. 7. This result is reflected in the slightly lower nucleation rate that is apparent in Fig. 12.

Discussion

As the velocity gradient in the laminar, stagnation point flow is increased, the gradients of the scalar quantities are increased, as seen in Fig. 4. Consequently, the rate of molecular mixing is enhanced. A high strain rate or velocity gradient in a laminar, stagnation point flame leads, eventually, to extinction of the flame as the rate of chemical reactions fails to keep up with the rate of mixing imposed by the flow.[7] Similarly, the strain rate has been found to have an impact on the formation of an aerosol in this numerical study.

Three processes are important in determining the dynamics of an aerosol. The first is homogeneous nucleation, which is capable of producing large numbers of particles very quickly. The second process is condensation onto existing particles. Finally, coagulation serves to decrease the number density of the aerosol. All of these processes may be affected by the flowfield if the strain rate is sufficiently high.

The residence time that particles have for condensational growth is proportional to the inverse strain rate, $1/a$ (s). With less time available for growth, the total mass of aerosol that is produced in the flow decreases with increasing strain rate.

As a result, less vapor is consumed by the condensation process. More vapor becomes available for nucleation, i.e., the supersaturation is increased.

Enhancement of the supersaturation by the reduction of condensational growth is due to a reduced convection time for particles. In addition, the rate of diffusion of vapor is greater at high strain rates because of the greater concentration gradients. At a velocity gradient of $10\ s^{-1}$, the gradient of water vapor mass fraction at the stagnation point is about $-0.04\ mm^{-1}$. At $1000\ s^{-1}$, the gradient is about $-0.39\ mm^{-1}$. The gradients scale with the square root of the velocity gradient. As a result of the steeper concentration gradient at the high velocity gradient, molecular diffusion is capable of sustaining high rates of nucleation by maintaining higher supersaturations.

A comparison of the nucleation rates for the two cases reveals that, at the high velocity gradient, the peak nucleation rate is 65 times greater than for the low velocity gradient case. However, the higher nucleation rate does not result in greater particle number densities near the stagnation point due to two offsetting factors, viz., the reduced residence time in the flow, which is determined by the velocity gradient and the effect of coagulation. The plot of particle number densities as a function of the nondimensional distance from the cylinder shows that they are approximately the same for both flows. It may be concluded that the velocity gradient does not affect this aspect of the aerosol characteristics.

The slower process of condensational growth is affected by the residence time in the vicinity of the stagnation point. Figure 8 reveals that the rates of condensation are about an order of magnitude greater for the low velocity gradient condition. This is primarily due to the larger size of particles and the concomitantly greater surface area that results from longer residence times for particles in the flow. The reduction in the vapor mass fraction and the supersaturation that lead to lower nucleation rates at low velocity gradients are too slight to affect the rate of condensation.

The range of velocity gradients that have been studied indicate a reduction in the mass fraction of condensate by two to three orders of magnitude (see Fig. 6). Because the particle diameters are governed by the mass fraction and the number density, one may conclude from these results that the particle diameters vary over a range of 5–10. The effect on light scattering may be significant. For infrared wavelengths, the particles may be close to the Rayleigh limit for light scattering for which their scattering efficiency varies with the particle volume. This quantity is in turn related directly to the condensate mass fraction. Consequently, significant effects on scattering could be expected as a result of variations in mixing rates. At shorter, visible wavelengths, the effect may not be quite as great but should nevertheless be observable. Furthermore, if the results of Fig. 6 were plotted vs distance from the cylinder, it would be apparent that the width of the aerosol layer is reduced by the high velocity gradient, i.e., the total amount of aerosol in the flow is reduced. This observation reinforces the conclusion that light scattering from the aerosol will be reduced at high strain rates.

Particles that were introduced into the flows outside the mixing layer in significant numbers appeared to have a modest effect on the dynamics of the aerosol. Only a small amount of vapor was consumed in condensation on the pre-existing particles and, as a result, the supersaturation was not reduced significantly. The rate of homogeneous nucleation was hardly affected and the particle number densities were reduced only slightly. In a uniform vapor, the presence of particles may suppress homogeneous nucleation altogether. In this flow, however, supersaturations are produced as the result of mixing, and if that process occurs sufficiently quickly, then there may not be adequate time for substantial conversion of vapor to liquid by relatively slow condensation. As a result, supersaturations may be produced that are significantly in excess of unity. The phenomenon may be compared to the behavior of the more familiar uniform vapor. In that case, supersaturations may be produced by changes in pressure via an expansion. If the process occurs sufficiently rapidly, then homogeneous nucleation is favored over the competing processes of heterogeneous nucleation or condensation.

The stagnation point flowfield that has been studied is relevant to the consideration of aerosol processes that may occur as the result of the turbulent mixing of different streams of gases. Velocity gradients or strain rates in the laminar flow may be interpreted in terms of the scalar dissipation rate of a turbulent flow; Bilger[8] has discussed how this quantity is associated with the rate of molecular mixing in a turbulent flow. The results that have been discussed here with regard to the effect of the stagnation flow strain rate on the aerosol dynamics may be applicable to flows that involve turbulent mixing.

Conclusions

A numerical model has been developed for the dynamics of an aerosol that is formed when a hot, moist gas stream meets a cooler, moist stream in a laminar, stagnation flow. Attention was given to the impact of the velocity gradient or strain rate of the flow on the dynamics of an aerosol.

An increase in the strain rate caused a reduction in the total mass of condensate that formed. This was due to a decrease in the residence time of particles in the flow. On the other hand, an increased strain rate resulted in an increase in the rate of formation of particles but did not cause an increase in the particle number density. This has been ascribed to the joint effect of reduced residence times for particle formation at higher velocity gradients and also to the effect of particle coagulation. The results suggest that rates of turbulent mixing may affect phenomena such as light scattering in aerosol forming flows.

Acknowledgment

The author is grateful for the support of a Unocal Foundation Award and an NSF Award CBTE-8857477.

References

[1]Amelin, A. G., Vishnepolskya, I. V., and Belyakov, M., "Experimental Investigations of the Speed of Homogeneous Condensation," *Journal of Aerosol Science*, Vol. 2, No. 2, 1971, pp. 93–102.

[2]Anisimov, M. P., and Cherevko, A. G., "Gas-Flow Diffusion Chamber for Vapour Nucleation Studies," *Journal of Aerosol Science*, Vol. 16, No. 2, 1985, pp. 97–107.

[3]Henry, J. F., Gonzalez, A., and Peters, L. K., "Dynamics of NH_4Cl Particle Nucleation and Growth at 253–296 K," *Aerosol Science Technology*, Vol. 2, No. 3, 1983, pp. 321–339.

[4]Gokoglu, S. A., and Rosner, D. E., "Thermophoretically Augmented Mass Transfer Rates to Solid Walls Across Laminar Boundary Layers," *AIAA Journal*, Vol. 24, No. 1, 1986, pp. 172–179.

[5]Meyer, J. W., "Kinetic Model for Aerosol Formation in Rocket Contrails," *AIAA Journal*, Vol. 17, No. 2, 1979, pp. 135–144.

[6]Batchelor, G. K. *An Introduction to Fluid Dynamics*, Cambridge University Press, Cambridge, UK, 1967.

[7]Tsuji, H., Progress in Energy and Combustion Science, Counterflow Diffusion Flames, Vol. 8, No. 2, 1982, pp. 93–119.

[8]Bilger, R. W., Progress in Energy Combustion and Science, Turbulent Jet Diffusion Flames, Vol. 1, No. 1, 1976, pp. 87–109.

[9]Springer, G. S., "Homogeneous Nucleation," *Advances in Heat Transfer*, Vol. 14, edited by T. F. Irvine and J. P. Hartnett, Academic, New York, 1978, pp. 281–346.

[10]Warren, D. R., and Seinfeld, J. H., "Nucleation and Growth of Aerosol from a Continuously Reinforced Vapor," *Aerosol Science Technology*, Vol. 3, No. 2, 1984, pp. 135–153.

[11]Fuchs, N. A., and Sutugin, A. G., *Topics in Current Aerosol Research*, Vol. 2, edited by G. M. Hidy and J. R. Brock, Pergamon, Oxford, England, UK, 1971, pp. 29–37.

[12]Gelbard, F., and Seinfeld, J. H., "The General Dynamic Equation for Aerosols," *Journal of Colloid Interface Science*, Vol. 68, No. 2, 1979, pp. 363–382.

[13]Smooke, M. D., "Solution of Burner-Stabilized Pre-Mixed Laminar Flames by Boundary Value Methods," *Journal of Computational Physics*, Vol. 48, No. 1, 1982, pp. 72–105.